



**HAL**  
open science

## **GDF5 as a rejuvenating treatment for age-related neuromuscular failure**

Massiré Traoré, Chiara Noviello, Amélie Vergnol, Christel Gentil, Marius Halliez, Lucile Saillard, Maxime Gelin, Anne Forand, Mégane Lemaitre, Zoheir Guesmia, et al.

► **To cite this version:**

Massiré Traoré, Chiara Noviello, Amélie Vergnol, Christel Gentil, Marius Halliez, et al.. GDF5 as a rejuvenating treatment for age-related neuromuscular failure. *Brain - A Journal of Neurology*, 2024, 147, pp.3834 - 3848. 10.1093/brain/awae107 . hal-04760455

**HAL Id: hal-04760455**

**<https://hal.science/hal-04760455v1>**



Submitted on 14 Nov 2024

**HAL** is a multi-disciplinary open access archive for the deposit and dissemination of scientific research documents, whether they are published or not. The documents may come from teaching and research institutions in France or abroad, or from public or private research centers.

L'archive ouverte pluridisciplinaire **HAL**, est destinée au dépôt et à la diffusion de documents scientifiques de niveau recherche, publiés ou non, émanant des établissements d'enseignement et de recherche français ou étrangers, des laboratoires publics ou privés.



# GDF5 as a rejuvenating treatment for age-related neuromuscular failure

Massiré Traoré,<sup>1,†</sup> Chiara Noviello,<sup>1,†</sup> Amélie Vergnol,<sup>1</sup> Christel Gentil,<sup>1</sup> Marius Halliez,<sup>1</sup> Lucile Saillard,<sup>1</sup> Maxime Gelin,<sup>1</sup> Anne Forand,<sup>1,2</sup> Mégane Lemaitre,<sup>3</sup> Zoheir Guesmia,<sup>1</sup> Bruno Cadot,<sup>1</sup> Eriky Caldas de Almeida Araujo,<sup>4</sup> Benjamin Marty,<sup>4</sup> Nathalie Mougenot,<sup>3</sup> Julien Messéant,<sup>1</sup> Laure Stochlic,<sup>1</sup> Jeremy Sadoine,<sup>5</sup> Lofti Slimani,<sup>5</sup> Ariane Jolly,<sup>6</sup> Pierre De la Grange,<sup>6</sup> Jean-Yves Hogrel,<sup>7</sup>  France Pietri-Rouxel<sup>1,‡</sup> and  Sestina Falcone<sup>1,‡</sup>

<sup>†,‡</sup>These authors contributed equally to this work.

Sarcopenia involves a progressive loss of skeletal muscle force, quality and mass during ageing, which results in increased inability and death; however, no cure has been established thus far. Growth differentiation factor 5 (GDF5) has been described to modulate muscle mass maintenance in various contexts.

For our proof of concept, we overexpressed GDF5 by AAV vector injection in tibialis anterior muscle of adult aged (20 months) mice and performed molecular and functional analysis of skeletal muscle. We analysed human vastus lateralis muscle biopsies from adult young (21–42 years) and aged (77–80 years) donors, quantifying the molecular markers modified by GDF5 overexpression in mouse muscle. We validated the major effects of GDF5 overexpression using human immortalized myotubes and Schwann cells. We established a preclinical study by treating chronically (for 4 months) aged mice using recombinant GDF5 protein (rGDF5) in systemic administration and evaluated the long-term effect of this treatment on muscle mass and function.

Here, we demonstrated that GDF5 overexpression in the old tibialis anterior muscle promoted an increase of 16.5% of muscle weight ( $P = 0.0471$ ) associated with a higher percentage of 5000–6000  $\mu\text{m}^2$  large fibres ( $P = 0.0211$ ), without the induction of muscle regeneration. Muscle mass gain was associated with an amelioration of 26.8% of rate of force generation ( $P = 0.0330$ ) and better neuromuscular connectivity ( $P = 0.0098$ ). Moreover, GDF5 overexpression preserved neuromuscular junction morphology (38.5% of nerve terminal area increase,  $P < 0.0001$ ) and stimulated the expression of reinnervation-related genes, in particular markers of Schwann cells (fold-change 3.19 for *S100b* gene expression,  $P = 0.0101$ ). To characterize the molecular events induced by GDF5 overexpression during ageing, we performed a genome-wide transcriptomic analysis of treated muscles and showed that this factor leads to a ‘rejuvenating’ transcriptomic signature in aged mice, as 42% of the transcripts dysregulated by ageing reverted to youthful expression levels upon GDF5 overexpression ( $P < 0.05$ ). Towards a preclinical approach, we performed a long-term systemic treatment using rGDF5 and showed its effectiveness in counteracting age-related muscle wasting, improving muscle function (17.8% of absolute maximal force increase,  $P = 0.0079$ ), ensuring neuromuscular connectivity and preventing neuromuscular junction degeneration (7.96% of AchR area increase,  $P = 0.0125$ ). In addition, in human muscle biopsies, we found the same age-related alterations than those observed in mice and improved by GDF5 and reproduced its major effects on human cells, suggesting this treatment as efficient in humans.

Overall, these data provide a foundation to examine the curative potential of GDF5 drug in clinical trials for sarcopenia and, eventually, other neuromuscular diseases.

- 1 Sorbonne Université, INSERM, Institut de Myologie, Centre de Recherche en Myologie, F-75013 Paris, France
- 2 Inovarion, F-75005 Paris, France
- 3 Sorbonne Université, INSERM UMS28, Phénotypage du Petit Animal, 75013 Paris, France
- 4 Institut de Myologie, CEA, Laboratoire d'imagerie et de spectroscopie par RMN, F-75013 Paris, France
- 5 Université de Paris, Plateforme d'Imagerie du Vivant (PIV), F-92120 Montrouge, France
- 6 GenoSplice, Paris Biotech Santé, F-75014 Paris, France
- 7 Institut de Myologie, Laboratoire de physiologie et d'évaluation neuromusculaire, F-75013 Paris, France

Correspondence to: Sestina Falcone  
Sorbonne Université, INSERM, Institut de Myologie  
Centre de Recherche en Myologie, 105 boulevard de l'Hôpital  
F-75013 Paris, France  
E-mail: s.falcone@institut-myologie.org

Correspondence may also be addressed to: France Pietri-Rouxel  
E-mail: france.pietri-rouxel@upmc.fr

**Keywords:** endplate; therapy; musculature

## Introduction

Sarcopenia is defined as a progressive age-related loss of strength, quality and mass of muscle inducing adverse outcomes, including frailty, disability and mortality.<sup>1</sup> Several mechanisms are proposed to explain the onset and progression of sarcopenia. Studies in rodents and humans suggest that age-related muscle denervation is a major driver of muscle fibre loss and force decline,<sup>2–4</sup> a phenomena not associated with motor neuron loss in the spinal cord, indicating that changes in the neuromuscular junction (NMJ) are key.<sup>5</sup> Perisynaptic Schwann cells (SCs), covering NMJs, play a critical role during their formation and maintenance, and are involved in neurotransmission and muscle reinnervation after peripheral nerve injury.<sup>6</sup> Interestingly, low reinnervation capacity observed in old muscle is associated with SC degeneration at the NMJ during ageing.<sup>7–10</sup>

Nevertheless, many factors are involved in age-related muscle changes, such as pro-inflammatory mediators and redox signalling imbalance, contributing to muscle wasting.<sup>11,12</sup> All these aspects must be considered from a therapeutic perspective for efficient treatment. Today, therapeutic approaches counteracting sarcopenia are limited to caloric restriction and physical exercise, which are met with limited patient compliance.<sup>13–17</sup> However, pharmacological strategies have been proposed,<sup>18</sup> based on myostatin and activin-A, modulators of muscle growth, to increase muscle mass,<sup>19</sup> but clinical trials showed no significant effect on muscle strength or physical performance of sarcopenic patients.<sup>19,20</sup> Other strategies are to: increase protein intake or vitamin D supplementation; inhibit interleukin-6 or tumour necrosis factor- $\alpha$  to reduce inflamm-aging; or administer hormones to enhance anabolism.<sup>21</sup> Nevertheless, none of these treatments alone rescue the neuromuscular failures characterizing sarcopenia.<sup>21</sup> Identification of novel drugs to counteract age-related neuromuscular failure is still challenging.

In this context, growth and differentiation factor 5 (GDF5) is of great interest because of its broad functions in the neuromuscular system.<sup>22–24</sup> GDF5 [also called bone morphogenetic protein (BMP) 14] belongs to the BMP family activating SMAD (fusion of *Caenorhabditis elegans* Sma and the *Drosophila* Mad, or mothers against decapentaplegic) 1/5 complex phosphorylation, leading to transcription of inhibitor of differentiation (Id) genes. BMPs are involved in bone and cartilage development and regeneration.<sup>25,26</sup>

Genetic polymorphisms and GDF5 mutations are associated with osteoarthritis susceptibility, joint and bone disorders<sup>27,28</sup> and also decreased muscle strength in humans over 65 years of age.<sup>29</sup> GDF5 can be considered a pleiotropic factor, modulating physiological processes to shape skeletal tissues, control angiogenesis,<sup>30</sup> trigger neuronal development and repair,<sup>31,32</sup> regulate adipose tissue metabolism<sup>33,34</sup> and, according to several studies, act as a neurotrophic factor.<sup>22,32,35,36</sup> Consistently, *Gdf5* transcription has been shown to be enriched at NMJ regions, and its receptors BMPR1A/BMPR1B expressed in muscle, motor nerve and nerve-associated cells.<sup>22</sup> After nerve damage, increased GDF5 expression has been shown to be essential to counteract atrophy,<sup>23</sup> sustain reinnervation<sup>22</sup> and regulate skeletal muscle mass homeostasis through signalling in mice.<sup>23,24,36–40</sup> Recently, we showed that age-related muscle mass loss is associated with the alteration of the compensatory mechanism involving GDF5 axis in mice and humans and that boosting this signalling prevents age-related muscle wasting.<sup>24</sup>

Here, we aimed to unravel the molecular mechanism underlying the beneficial effects of GDF5-based strategies on neuromuscular features during ageing. We showed that local GDF5 overexpression (OE) in mice, initiated at the onset of age-related muscle atrophy, increased muscle mass and function, inhibited protein degradation and ameliorated neuromuscular connectivity and NMJ morphology. This effect was associated with muscle reinnervation likely linked to SCs. Whole-transcriptome sequencing of adult/aged muscle overexpressing GDF5 demonstrated a 'rejuvenating' transcriptomic signature in GDF5-treated aged muscles compared to adult/aged controls. To translate this finding to humans, we used systemic administration of recombinant GDF5 protein (rGDF5) in mice and demonstrated its benefits in preventing age-related neuromuscular failure involving muscle mass and function, as well as an age-dependent decrease in the levels of SC-specific markers in human muscle biopsies, strongly suggesting GDF5 administration to promote SC maintenance. Importantly, we provide evidence of human synthetic GDF5 (hsGDF5) effectiveness in inducing human SC proliferation and decreasing MuRF1-ubiquitin ligase expression in human muscle cells.

Altogether, our findings shed light on the benefits of GDF5-based therapies for the neuromuscular system and are the basis of forthcoming medical strategies to counteract sarcopenia and other neuromuscular diseases in humans.

## Materials and methods

### Ethics

Animal experimental procedures were approved by the ethics committee (MENESR: Project #17975). For human muscle biopsies, we received ethical approval, and participants provided written informed consent.

### Animals

Adult (6/7 months), old (20 months) and very old (26–27 months) C57/BL6 female mice were obtained from the Janvier Lab and housed under specific-pathogen-free (SPF) conditions.

### Human muscle biopsies

Human vastus lateralis biopsies from adult/aged healthy volunteers (Supplementary Table 1) were gathered within the framework of the European project MyoAge<sup>41</sup> (223576-FP7-HEALTH) and by the Institute of Myology Myobank (BB-0033-00012).

### Cell culture

The hTERT-NF1 cells were cultured in Dulbecco's modified Eagle medium (DMEM) containing 10% fetal bovine serum (FBS) and 0.1% gentamicin and treated for 48 h with PBS or hsGDF5 (X'PROCHEM) at 10 or 50 ng/ml. Cell proliferation was determined by spectrofluorometry (CytoQuant assay, Life Technologies).

Human healthy immortalized myoblasts (8220 cells)<sup>42</sup> proliferated in DMEM, 5 µg/ml insulin, 5 ng/ml EGF, 0.5 ng/ml bFGF, 0.2 µg/ml dexamethasone, 25 µg/ml fetuin, 20% FBS and 16% medium 199; differentiated for 5 days in IMDM, 2% hydrogen sulphide (HS),<sup>42</sup> then treated for 72 h with hsGDF5 (50 ng/ml) or PBS.

### In vivo gene transfer

AAV2/1 (adeno-associated virus) vectors were prepared as described.<sup>43</sup> AAV2/1-Scramble (-Scra) or -GDF5 were injected in tibialis anterior (TA) muscle of old (20 months) mice at 5.10<sup>9</sup>vg/TA. Further details are provided in the Supplementary material.

### Recombinant GDF5 administration

Twenty-month-old mice were injected intraperitoneally thrice a week for 4 months with mouse rGDF5 (Merck) or vehicle [PBS-0.1% bovine serum albumin (BSA)].

### Haematoxylin and eosin staining

Muscle cryosections (10 µm) were fixed on glass slides in 4% paraformaldehyde (PFA) and stained with haematoxylin (BIOGNOST) and eosin (ScyTek Lab).

### Immunofluorescence

Cryosections were fixed in 4% PFA, permeabilized with 0.5% Triton X-100 and blocked in 10% HS, 0.2% Triton, 5% BSA-PBS and incubated overnight at 4°C with primary antibodies (Supplementary Table 6). Sections were incubated with secondary antibodies (Supplementary Table 7) for 1 h at room temperature and mounted with Fluoromont-G (Invitrogen). Further details are provided in the Supplementary material.

### Neuromuscular-junction morphology

Isolated muscle fibres were fixed for 1 h in 4% PFA, blocked in 4% BSA, 5% goat serum, 0.5% Triton-PBS and incubated overnight at 4°C with Neurofilament antibody (Supplementary Table 6). After washes in 0.1% Triton-PBS, fibres were incubated overnight at 4°C with a secondary antibody (Supplementary Table 7) and  $\alpha$ -Bungarotoxin-Alexa Fluor<sup>TM</sup>-594. Isolated fibres were mounted on glass slides with mounting medium. Further details are provided in the Supplementary material.

### Immunoblotting

Muscle cryosections (400 µm) were homogenized (Dounce) in lysis buffer (Ozyme)/phosphatase inhibitors (Roche). Proteins were denatured at 95°C for 5 min with Laemmli buffer, separated by electrophoresis (Nu-PAGE 4–12% Bis-Tris gel) and transferred to nitrocellulose membranes. Membranes were blocked with 5% milk or 5% BSA and incubated overnight at 4°C with primary antibodies (Supplementary Table 6). Membranes were incubated with secondary antibodies (Supplementary Table 7). Images were acquired with ChemiDoc<sup>TM</sup> MP (Bio-Rad), and the band intensity was quantified using Image Lab software (Bio-Rad).

Protein synthesis was measured using the *in vivo* surface sensing of translation (SUnSET) method, followed by immunoblotting<sup>44,45</sup>

### RNA-sequencing

Messenger RNA libraries were realized following the manufacturer's recommendations (Ultra2 mRNA, New England Biolabs). Twelve sample-pooled library preparations were sequenced on a Novaseq6000 system from Illumina with SP-200 cycles/cartridge (2 × 800 million 100 base reads). Further details are provided in the Supplementary material.

### RNA isolation and real-time quantitative PCR

Total RNA was extracted from muscle using TRIzol/Direct-zol RNA MiniPrep w/Zymo-Spin IIC Columns (Ozyme) and from cells using NucleoSpin RNA Columns (Macherey-Nagel). Reverse transcription was performed using a SuperScript II Reverse Transcriptase kit (Thermo Fisher Scientific), and real-time quantitative PCR (RT-qPCR) was performed on a StepOne Plus Real-Time PCR System (Applied Biosystems) using Power SYBR Green PCR MasterMix (Thermo Fisher Scientific). Data were analysed using the  $\Delta\Delta$ CT method and normalized to RPLP0 (ribosomal protein lateral stalk subunit P0) or, for hTERT NF1 cells, GAPDH (glyceraldehyde 3-phosphate dehydrogenase) expression. Primers are listed in Supplementary Table 8.

### In situ muscle force and electroneuromyography measurements

Muscle force was evaluated by measuring *in situ* TA muscle contraction after nerve stimulation<sup>24</sup> and electroneuromyography (ENMG) was achieved in TA muscle.<sup>46</sup> Further details are provided in the Supplementary material.

### Grip strength

We used a grip strength meter (Bioseb) to assess hind- and fore-limb strength. Mice were lifted, held by the tail and gently pulled backwards until they released the grid. The mean of four

consecutive measurements was determined and normalized to body weight.

## MRI

The MRI system consisted of a 7 T Bruker BioSpec and a transceiver surface cryoprobe (Bruker BioSpin MRI GmbH). Maximal muscle cross-sectional area (CSA) was determined with ITK-SNAP software.<sup>47</sup> Further details are provided in the [Supplementary material](#).

## Whole metabolism exploration and body composition

Mice were housed individually in metabolic cages (Labmaster, TSE systems GmbH) with *ad libitum* access to food and water. They were acclimated for 4 days before monitoring for the next 3 days. O<sub>2</sub> consumption, CO<sub>2</sub> production, energy expenditure and respiratory exchange ratio were measured using the indirect calorimetry technique. Food and water intake and spontaneous locomotor activity were recorded during the entire experiment. Lean and fat masses were assessed using 7.5-MHz time-domain-nuclear magnetic resonance (LF90II MiniSpec; Bruker).

## Echocardiography

Mice were lightly anaesthetized (0.2%–0.5% isoflurane), and ECG was performed on a 37°C pad with a probe emitting ultrasound at a frequency of 9–14 MHz (Vivid7 PRO apparatus; GE Medical System) applied to the chest wall. Cardiac ventricular dimensions and fractional shortening were measured in 2D mode and M-mode.

## Bone micro-CT

Dried mouse femurs were scanned using *in vivo* high-resolution X-ray micro-CT instrument (Quantum FX Caliper, Life Sciences, Perkin Elmer) hosted by the Life Imaging Facility (URP2496, Montrouge, France). Further details are provided in the [Supplementary material](#).

## Statistics analyses

Comparison between two groups was tested for normality using the Shapiro–Wilk test followed by parametric (two-tailed paired, unpaired Student's *t*-test) or non-parametric test (Mann–Whitney) to calculate *P*-values. For more than two groups, ordinary one or two-way ANOVA tests followed by appropriated *post hoc* tests were performed. All statistical analyses were performed with GraphPad Prism 8 software and statistical significance was set at *P* < 0.05.

## Results

### GDF5 overexpression prevents neuromuscular system decline during ageing in mice

We characterized neuromuscular features by analysing parameters defining muscle mass and function and denervation markers in younger adult (7 months), old (20 months) and very old (26–27 months) mice. We found that from 20 months, the masses of the TA and gastrocnemius (GAS) were progressively reduced, without significant body weight loss ([Fig. 1A](#)), whereas extensor digitorum longus (EDL) and soleus (SOL) were less affected by ageing ([Supplementary Fig. 1A](#)). Muscle fibre quantification revealed a diminution of fibre size ([Supplementary Fig. 1B](#)), particularly of

fast-twitch glycolytic MyHC-IIB fibres but not a reduction in their number ([Supplementary Fig. 1C](#)).

To establish whether muscle atrophy was associated with impaired function, we measured limb muscle grip strength, *in situ* tetanic force generation and *in vivo* neuromuscular transmission by ENMG assessing compound muscle action potentials (CMAPs).<sup>48,49</sup> We found that grip strength was diminished early in old as well as very old compared with younger (7-month-old) mice ([Fig. 1B](#)); and absolute maximal force generated by TAs was lower in very old mice, while not different between older and younger adult animals ([Supplementary Fig. 1D](#)). Nevertheless, we found no difference in tetanic force normalized to TA weight, meaning that force generation was directly dependent on muscle mass. Interestingly, we measured a slower rate of force production in muscles of very old mice, indicating contractile system impairment<sup>50</sup> ([Supplementary Fig. 1D](#)). Consistently, ENMG revealed a CMAP decrement in very old mice ([Fig. 1C](#)), evidencing neuromuscular fatigability in these animals.<sup>48</sup> Altogether, these results showed that ageing affects muscle contractility and neuromuscular function without modifying specific force generation.

To assess NMJ denervation in aged muscle, the mRNA expression of related markers such as acetylcholine receptor (AChR) subunits (*Chrna1*, *-b1*, *-d*, and *-g*) and *Musk*<sup>10,24</sup> was measured. We observed a trend towards increased expression of most of these markers beginning at 20 months, while *Chrn**g* levels were significantly higher (*P* = 0.0429) in very old mice ([Fig. 1D](#)), suggesting the presence of NMJ instability and/or remodelling beginning in old mice.

Altogether, these data revealed that muscle mass loss precedes alterations in force generation and neuromuscular connectivity during ageing.

### GDF5 overexpression stimulates muscle hypertrophy and protein synthesis in old mice

Our findings could define a time window to take action with therapeutic strategies to prevent signs of sarcopenia. To this aim, we injected TAs of 20-month-old mice with AAV-GDF5 or -Scra and analysed these muscles 4 weeks after injection ([Fig. 1E](#)). First, transcript and protein GDF5-OE was confirmed by RT-qPCR and western blotting (WB), respectively ([Supplementary Fig. 1E](#)). GDF5-dependent signalling activation was validated by the quantification of a higher number of phosphorylated SMAD1/5-positive nuclei after AAV-GDF5 than after AAV-Scra injection by immunofluorescence. Accordingly, transcription of *Id1*, 2, 3 and 4 GDF5 gene targets<sup>24,51,52</sup> was induced upon GDF5-OE ([Supplementary Fig. 1F](#)). Analysis of muscle weight, fibre size and number showed hypertrophy of GDF5-OE TAs ([Fig. 1E](#)) with a higher percentage of large fibres without fibre number change ([Fig. 1F](#)). The regeneration process was not involved in mass gain as quantification of the number of myonuclei, indicating muscle cell proliferation, and of the centrally nucleated fibre, showed no variation in GDF5-OE muscle compared to control ([Fig. 2A](#)). Furthermore, the expression of satellite cell marker *Pax7*<sup>53</sup> and of myogenic regulatory factors *MyoD*, *myogenin* and *Myf6*<sup>53</sup> was not modified by GDF5-OE ([Fig. 2B](#)). Finally, to establish whether GDF5 could target specific fibre type size, we measured the CSA of MyHC-IIA-, MyHC-IIB- and MyHC-IIX-positive fibres, without finding difference in the mean size of any single type ([Supplementary Fig. 2A and B](#)). These results suggest that GDF5-OE leads to hypertrophy of muscle at the early stage of ageing.

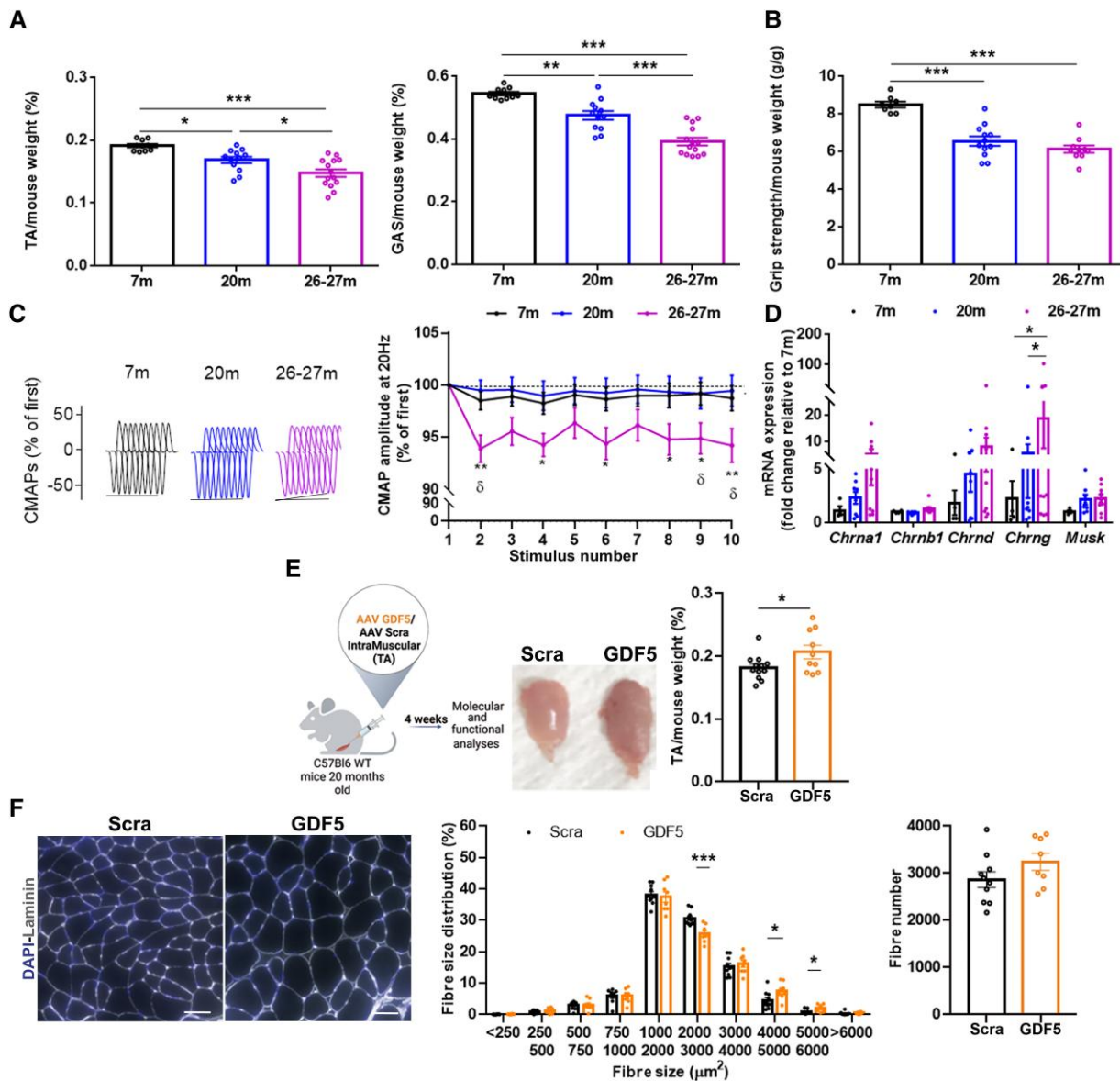


**Figure 1** Age-related neuromuscular failure and GDF5 overexpression in muscle. (A) Weight of tibialis anterior (TA) and gastrocnemius (GAS) of adult (7 months;  $n = 10$ ), old (20 months;  $n = 12$ ) and very old (26–27 months;  $n = 14$ ) mice normalized to body weight. (B) Grip strength mean of adult ( $n = 8$ ), old ( $n = 12$ ) and very old ( $n = 10$ ) mice normalized to body weight. (C) Representative electromyography traces recorded in TAs across ages and amplitudes of compound muscle action potentials (CMAPs) (adult  $n = 11$ ; old  $n = 12$ ; very old  $n = 16$ ). (D) Real-time quantitative PCR for *Chrna1*, *Chrb1*, *Chrnd*, *Chrn1g* and *Musk* in TAs across ages (adult  $n = 4$ ; old  $n = 8$ ; very old  $n = 9$ ). (E) Experimental design: AAV-Scramble (Scra) or -GDF5 (GDF5) were injected in 20-month-old mouse TA (created with BioRender.com). Representative picture of TAs injected for 4 weeks with Scra or GDF5 (21-month-old). Weight of TAs was normalized to body weight (Scra  $n = 12$ ; GDF5  $n = 10$ ). (F) Representative images of 21-month-old TAs injected with Scra or GDF5, immunostained with laminin (staining membrane) and DAPI (staining nuclei); scale bar = 100  $\mu\text{m}$ . Size distribution of TA fibres and mean myofibre number were determined in Scra ( $n = 10$ ) or GDF5 ( $n = 8$ ) conditions. All data are mean  $\pm$  standard error of the mean. \* $P < 0.05$ , \*\* $P < 0.01$ , \*\*\* $P < 0.001$ . (A–D)  $P$ -values were calculated by ordinary one-way ANOVA followed by Tukey's multiple comparison test or (E and F) unpaired t-test.

Since muscle mass homeostasis is regulated by the balance between protein degradation and synthesis,<sup>54</sup> we determined active protein synthesis after GDF5-OE by *in vivo* SunSET assay.<sup>17</sup> We found increased puromycin incorporation into GDF5-OE TA extracts (Fig. 2C), indicating that hypertrophy might be partially due to increased anabolism. However, we did not observe AKT/m-TOR/RpS6 phosphorylation, canonically associated with protein synthesis<sup>55</sup> (Fig. 2D and Supplementary Fig. 2C). To investigate protein breakdown, we quantified the mRNA expression of atrogenes such as *MuRF1*, *Atrogin1* and *Musa1*<sup>23</sup> and showed a significant decrease ( $P = 0.0437$ ) in only the *MuRF1* transcript level in GDF5-OE

TAs (Fig. 2E). Accordingly, we observed increased levels of MyHC and actin, two proteins directly targeted by *MuRF1*<sup>56,57</sup> for degradation and higher  $\alpha$ -actinin protein level also reported as associated with *MuRF1* downregulation<sup>58</sup> in GDF5-OE TAs compared to scramble (Fig. 2F). In addition, to explore eventual effect of GDF5-OE on the proteasome-ubiquitin system, we quantified protein poly-ubiquitination<sup>59</sup> and found a decrease in its levels in GDF5-OE TA extracts versus scramble (Fig. 2G), indicating a global inhibitory effect of GDF5 against proteasome-ubiquitin-dependent protein degradation. The autophagy/mitophagy pathway has been described as contributing to proteostasis and being deregulated

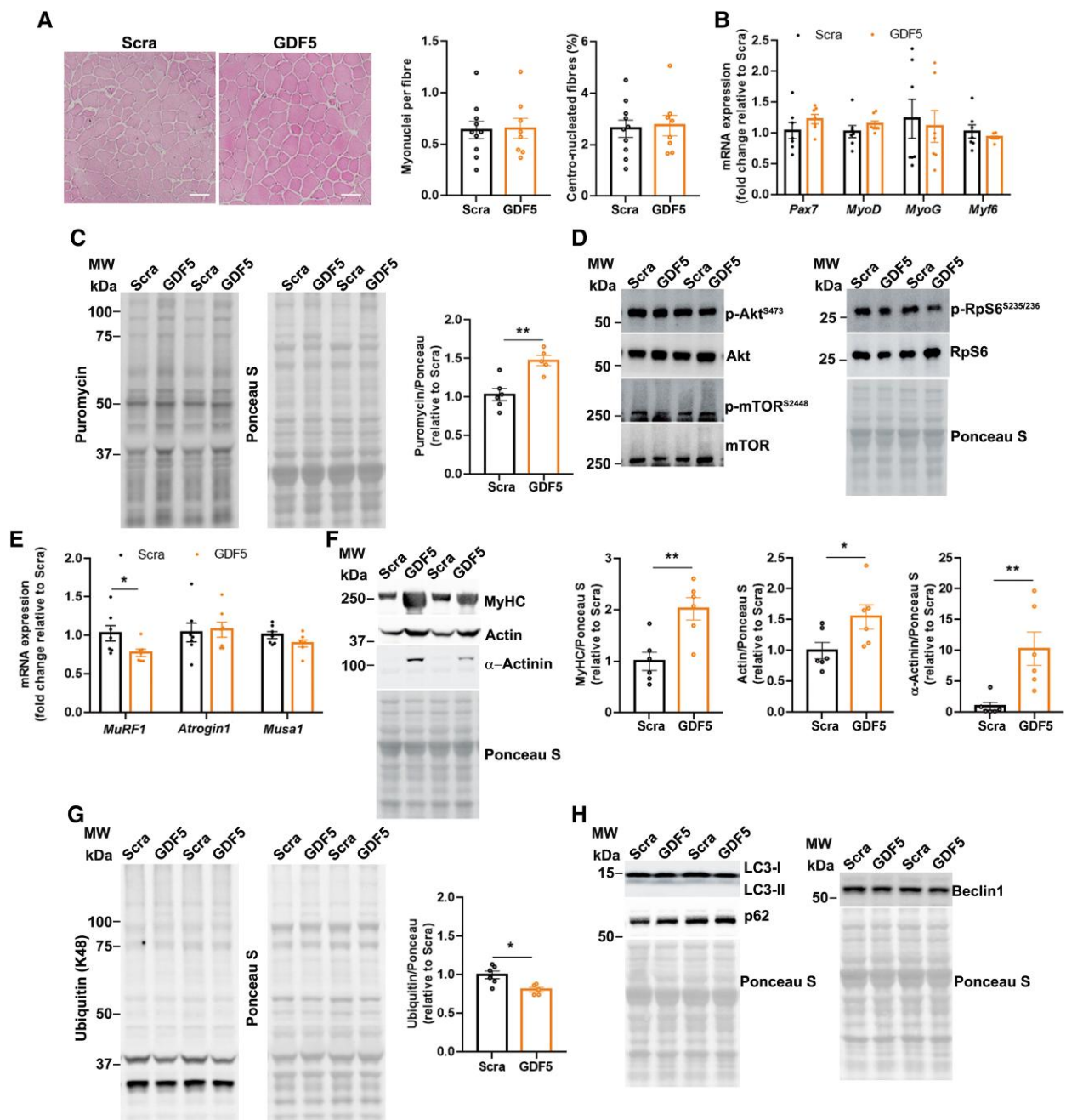


**Figure 2** Local GDF5 overexpression in old mice leads to muscle hypertrophy. (A) Representative images of tibialis anterior (TA) cryosections from 21-month-old mice injected with AVV-Scramble (Scra) or -GDF5 (GDF5), stained with haematoxylin and eosin; scale bar = 100  $\mu$ m. Number of myonuclei per fibre and proportion of centro-nucleated fibres were determined using an ImageJ-based machine learning algorithm (Scra  $n = 10$ ; GDF5  $n = 8$ ). (B) Real-time quantitative PCR (RT-qPCR) for *Pax7*, *Myod*, *Myog* and *Myf6* analysed in TAs injected with Scra ( $n = 7$ ) or GDF5 ( $n = 7$ ). (C) Representative western blot showing the level of puromycin-labelled proteins in TAs injected with Scra or GDF5. Relative signal intensity of puromycin-labelled proteins was determined (Scra  $n = 6$ ; GDF5  $n = 5$ ). Ponceau S staining was used as loading control. (D) Representative western blot showing the level of phosphorylated and total Akt, m-TOR and Rps6 proteins in TAs injected with Scra or GDF5. (E) RT-qPCR for *MuRF1*, *Atrogin1* and *Musa1* analysed in TAs injected with Scra ( $n = 7$ ) or GDF5 ( $n = 7$ ). (F) Representative western blot showing the level of MyHC, Actin and  $\alpha$ -Actinin proteins in TAs injected with Scra or GDF5. Relative signal intensity of proteins was determined (Scra  $n = 6$ ; GDF5  $n = 6$ ). Ponceau S staining was used as loading control. (G) Representative western blot showing the level of ubiquitinated proteins in TAs injected with Scra or GDF5. Relative signal intensity of ubiquitinated proteins was determined (Scra  $n = 6$ ; GDF5  $n = 5$ ). Ponceau S staining was used as loading control. (H) Representative western blot showing the levels of LC3-I, LC3-II, p62 and Beclin1 proteins in TAs injected with Scra or GDF5. Ponceau S staining was used as a loading control. All data are shown as the mean  $\pm$  standard error of the mean. \* $P < 0.05$ , \*\* $P < 0.01$ , \*\*\* $P < 0.001$ . (A–H)  $P$ -values were calculated by unpaired  $t$ -test. MW = molecular weight.

during ageing.<sup>60,61</sup> We thus investigated the gene expression of autophagic markers sequestome 1 (*p62* also known as SQSTM1), microtubule-associated protein 1A/1B-light chain 3 (*lc3b*), gamma-aminobutyric acid receptor-associated protein-Like 1

(*Gabarapl*), beclin 1 (*Becn1*), Bcl-2/adenovirus E1B 19 kDa protein-interacting protein 3 (*Bnip3*) and lysosomal cathepsin L<sup>62</sup> as well as the protein levels of lipidated LC3 (LC3-I/LC3-II), p62/SQSTM1 and Beclin1, of which an increase is associated with autophagy/

mitophagy activation.<sup>61</sup> We showed that GDF5-OE did not induce muscle mass gain through modifications in gene (Supplementary Fig. 2D) and protein expression of all these autophagy/mitophagy players (Fig. 2H and Supplementary Fig. 2E).

Here, our data revealed that the GDF5-OE hypertrophic effect is promoted by Akt/mTOR-independent protein synthesis and by the inhibition of MuRF1 and ubiquitin-dependent protein degradation without modulation of autophagy/mitophagy.

### GDF5 overexpression improves neuromuscular transmission, NMJ morphology and SC marker expression

To investigate the effects of GDF5 on muscle contraction through NMJ stimulation, we measured the peak of tetanic force and the rate of force generation in old mouse TAs. We found no difference in absolute or specific maximal force after nerve stimulation between GDF5-OE and scramble conditions. However, the rate of muscle force production was higher after GDF5-OE, indicating a faster development of contraction<sup>63</sup> than in scramble (Fig. 3A and Supplementary Fig. 3A). In addition, ENMG confirmed that GDF5 improved CMAP in old mice (Fig. 3B), showing that one of its major effects is the maintenance of neuromuscular transmission.

These results provided an extensive description of the effects of GDF5-OE during the earliest phase of age-related muscle wasting and validated its effectiveness in modulating neuromuscular function.

The evidence of the GDF5-OE benefit to NMJ activity strongly suggested its impact on NMJ remodelling. Thus, we analysed the morphology of muscle synapses using an ImageJ-based workflow<sup>64</sup> and found that GDF5-OE improved NMJ morphology in 21-month-old mice by a slight increase of endplate area ( $P=0.0577$ ) associated with a significant rise of AChR area ( $P=0.0145$ ). The presynaptic compartment showed increased nerve terminal area and pre- and post-synaptic overlap percentage (Fig. 3C). However, AChR compactness and fragmentation were not significantly affected (Supplementary Fig. 3B), nor was the expression of *Chrmg*, one of the hallmarks of NMJ instability/remodelling (Supplementary Fig. 3C).

To assess the effects of GDF5 on NMJ players, we quantified the transcript levels of the SC-specific glial markers, *S100b*, myelin basic protein (*Mbp*), myelin protein zero (*Mpz*) and peripheral myelin protein 22 (*Pmp22*) related to SC-dependent endplate stability<sup>65–68</sup>; growth-associated protein 43 (*Gap43*) associated with axon and SC regeneration; and fibroblast growth factor binding protein-1 (*Fgfbp1*), a trophic factor protecting NMJs from degradation.<sup>10,65,68</sup> Strikingly, we found that GDF5 increased the mRNA levels of all of them (Fig. 3D). To investigate whether this was accompanied

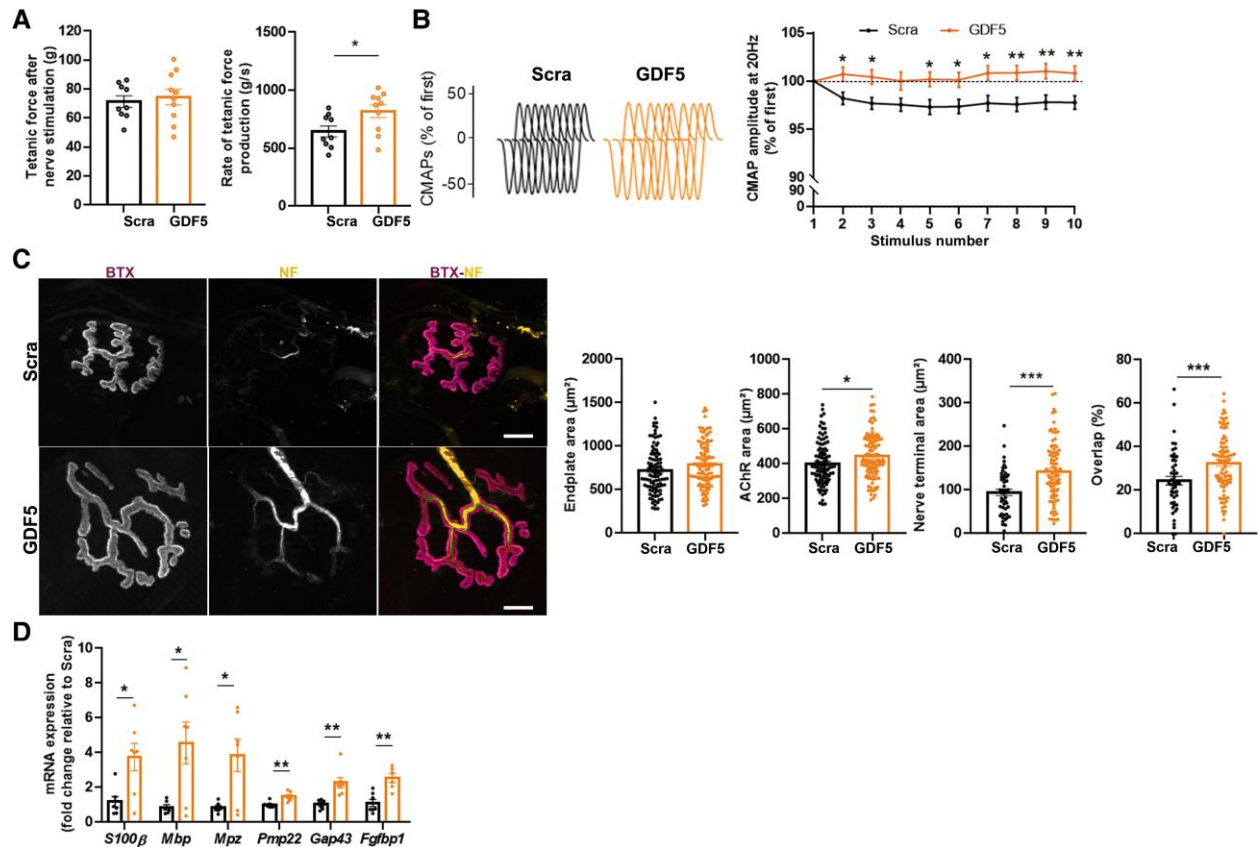


**Figure 3** GDF5 overexpression improves neuromuscular connectivity and neuromuscular junction morphology. (A) Absolute tetanic force and rate of force production measured in tibialis anterior (TA) from 21-month-old mice injected with AAV-Scramble (Scra  $n=9$ ) or -GDF5 (GDF5  $n=10$ ). (B) Representative electroneuromyography (ENMG) traces and CMAPs amplitudes recorded in TAs injected with Scra ( $n=9$ ) or GDF5 ( $n=10$ ). (C) Representative images of neuromuscular junction from TAs injected with Scra or GDF5, immunostained with neurofilament (NF: staining nerve terminal) and bungarotoxin (BTX: staining acetylcholine receptor); scale bar = 10  $\mu\text{m}$ . Endplate area, acetylcholine receptor (AChR) area, nerve terminal area and overlap (nerve terminal area/AChR area ratio) parameters were determined in Scra ( $n=4$ ) or GDF5 ( $n=3$ ) using an ImageJ-based workflow. (D) Real-time quantitative PCR for *S100 $\beta$* , *Mbp*, *Mpz*, *Pmp22*, *Gap43* and *Fgfbp1* analysed in TAs injected with Scra ( $n=6$ ) or GDF5 ( $n=6$ ). All data are shown as the mean  $\pm$  standard error of the mean. \* $P < 0.05$ , \*\* $P < 0.01$ , \*\*\* $P < 0.001$ . (A, B and D)  $P$ -values were calculated by unpaired t-test or (C) by Mann-Whitney test.



by changes in neurotrophic gene expression, we measured nerve growth factor (*Ngf*), brain-derived neurotrophic factor (*Bdnf*), neurotrophin 3 (*Nt3*), glial cell line-derived neurotrophic factor (*Gdnf*) and ciliary neurotrophic factor (*Cntf*) transcript levels. We observed that GDF5-OE increased *Ngf* expression (Supplementary Fig. 3D), suggesting that its effect might also be mediated by this neurotrophin involved in axon maintenance/guidance.<sup>66</sup>

Overall, our data showed that GDF5-OE benefits the integrity of NMJs and modulates SC markers and *Ngf* expression, indicating its therapeutic interest for disorders involving SCs and/or axonal degeneration as peripheral demyelinating neuropathies.

### Aged human muscle is a potential target of GDF5-based therapies

We investigated whether GDF5-based therapy could be useful against sarcopenia in humans. For that purpose, we collected biopsies from quadriceps of adult young (21–42 years) and aged (77–80 years) volunteers<sup>24</sup> (Supplementary Table 1) and assessed some relevant readouts established in mice. First, the expression of SC-related markers was measured, revealing *S100b* and MPZ mRNA levels significantly lower in aged than in young muscle biopsies ( $P = 0.0396$  and  $P = 0.0166$ , respectively) (Fig. 4A). We then treated human immortalized SCs with 10 and 50 ng/ml of human synthetic GDF5 (hsGDF5) for 48 h (Fig. 4B) and observed a significant increased rate of their proliferation ( $P = 0.0002$  and  $P < 0.0001$ , respectively), as evaluated by spectrofluorometry and RT-qPCR quantification of *Ki67* expression (Fig. 4B). In addition, hsGDF5 induced the differentiation of these cells, as confirmed by the increased mRNA levels of early myelin-associated markers early growth response gene 2 (*EGR2*), proteolipid protein 1 (*PLP1*), and *PMP22* (Fig. 4C). However, the expression of MPZ and MBP, mature myelinating SC markers, did not change under the tested conditions (Supplementary Fig. 4A). Altogether, these data strongly suggested a direct GDF5 effect on SCs playing fundamental roles in sustaining NMJ formation and preservation.<sup>69</sup>

One of the relevant effects of GDF5 on aged mouse muscle mass wasting was decreased *MuRF1* expression. We treated differentiated human immortalized myotubes with hsGDF5 for 72 h and found significantly decreased *MuRF1* expression ( $P = 0.0125$ ), confirming the ability of GDF5 to inhibit this protein breakdown mediator in human muscle cells (Fig. 4D).

These results provide evidence of GDF5's therapeutic potential in humans and identify the probable targets of the treatment as both SCs and muscle cells, crucial for neuromuscular connectivity and muscle mass.

### GDF5 overexpression rejuvenates transcriptomic profile in aged mouse muscle

To decipher the effects of GDF5-OE in muscle, we performed a genome-wide transcriptomic analysis using RNA from TAs of 21-month-old mice overexpressing GDF5 (Old-GDF5) compared to RNA from scramble-injected TAs of 7-month-old (Adult-Scra) and 21-month-old mice (Old-Scra) (Supplementary Tables 2 and 3). Principal component analysis revealed distinct gene-expression profiles among groups; however the Old-GDF5 group clustered more with the Adult-Scra than the Old-Scra group (Fig. 5A), and this was confirmed by unsupervised, hierarchical clustering analysis (Fig. 5B). Remarkably, of 587 genes affected by ageing, 247 genes differentially expressed in the Old-Scra reverted to youthful expression levels in the Old-GDF5 (42% of the dysregulated

transcripts) (Fig. 5C and Supplementary Table 4). This reversal was also observed for the expression of macrophage-specific as well as mitochondrial metabolism- and redox balance-related genes, the alterations of which have been reported to contribute to skeletal muscle disorders and ageing.<sup>70–73</sup>

To validate these data, we quantified by RT-qPCR the expression of some of most relevant genes modulated upon GDF5-OE in RNA extracts used for transcriptomic analysis. Among macrophage-associated genes, in the Old-GDF5 group, we observed upregulation of monocyte-macrophage marker colony stimulating factor 1 receptor (*Csf1r*)<sup>74</sup> and M2 anti-inflammatory macrophage markers *Cd163*, *Cd209* and *Mgl2* (Fig. 5D), known to support tissue repair and muscle mass maintenance.<sup>75,76</sup> In addition, GDF5-OE improved the expression of uncoupling protein2 (*Ucp2*)<sup>77–79</sup> and superoxide dismutase 3 (*Sod3*)<sup>80</sup> genes, implicated in energy expenditure, and negative regulator of reactive oxygen species (*Nrros*), limiting reactive oxygen species generation and oxidative damage (Fig. 5D).<sup>81</sup> We also found increased levels of other markers not altered by ageing, such as *F4/80*, *CD68*, *CD206* (macrophage markers), and catalase, *Gpx1* and *Hmox1* (antioxidant-related genes) (Supplementary Fig. 5A), suggesting that these modulations are applicable to GDF5 protective function against muscle wasting. Interestingly, apelin and follistatin expression, both described as beneficial in preventing age-related muscle decline and secreted after physical exercise,<sup>17,82,83</sup> was increased upon GDF5-OE (Fig. 5E). We also investigated the expression of *PGC-1 $\alpha$* , another factor involved in oxidative energy balance, exercise adaptation, myokine modulation and NMJ formation.<sup>84,85</sup> We found that *PGC-1 $\alpha$*  transcription was not modified upon GDF5-OE under our experimental conditions (Supplementary Fig. 5B).

To go further, as mitochondrial alterations are associated to sarcopenia,<sup>86</sup> we analysed mitochondrial content and morphology in TAs overexpressing GDF5. We did not measure significant changes in mitochondrial DNA amount and succinate dehydrogenase complex subunit A (*SdhA*-Complex II), cytochrome b-c1 complex subunit 2 (*Uqcrc*-Complex III) and voltage-dependent anion selective channel (*Vdac*) protein expression (Supplementary Fig. 5C and D), nor in the volume and gross morphology of mitochondria (Supplementary Fig. 5E). Accordingly, the expression of dynamin-related protein 1 (*Drp1*), fission 1 protein (*Fis1*), optic atrophy 1 (*Opa1*) and mitofusin 1 and 2 (*Mfn1/Mfn2*), regulating mitochondrial fission and fusion,<sup>87</sup> was not modified by GDF5-OE (Supplementary Fig. 5F).

These results represent an important dataset on the wide therapeutic potential of GDF5 in modulating various mechanisms contributing to muscle ageing and its involvement in several muscular and neuromuscular diseases.

### Recombinant mouse GDF5 is a potential therapy for age-related muscle wasting

With the goal of generating patient-relevant preclinical data to be used against sarcopenia, we set up a protocol based on recombinant mouse GDF5 protein (rGDF5). We treated old mice (20 months) with rGDF5 (0.2 mg/kg) or vehicle thrice a week systemically (Fig. 6A) as we validated that SMAD1/5 signalling was activated in TAs 48 h post-injection (Supplementary Fig. 6A). Four weeks later, we evaluated the expression of genes related to reinnervation and myokines and analysed the long-term effect of the treatment on age-related muscle wasting and neuromuscular features (Fig. 6A). We observed SC marker upregulation, including *S100b*, *Mbp*, *Mpz*, *Gap43* and also *Gfbbp1* and *Ngf*, as well as

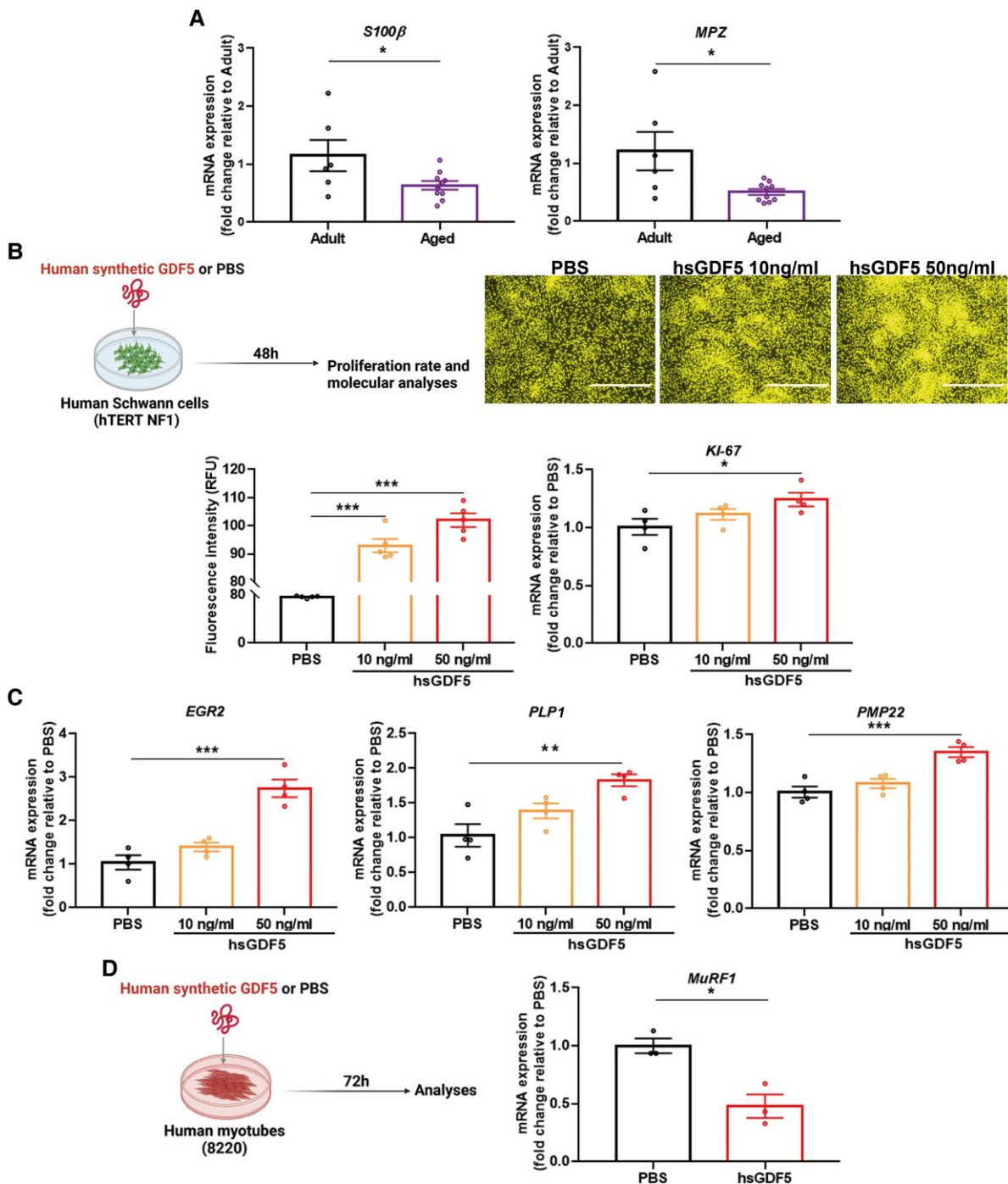


**Figure 4** Human synthetic GDF5 enhances human Schwann cell proliferation and decreases MuRF1 expression in human muscle cells. (A) Real-time quantitative PCR (RT-qPCR) for *S100β* and *MPZ* analysed in human quadriceps biopsies from Adult (21–42 years;  $n = 6$ ) and Aged (77–80 years;  $n = 10$ ) healthy volunteers. (B) Graphical representation of *in vitro* experiment (created with BioRender.com). Human Schwann cells (hTERT NF1) were treated with human synthetic GDF5 (hsGDF5) or PBS (control) and 48 h after the rate of cell proliferation and gene expression experiments were performed. Representative images showing hTERT NF1 cell nuclei after treatment for 48 h with PBS or hsGDF5 at 10 or 50 ng/ml; scale bar = 100  $\mu$ m. hTERT NF1 cell proliferation rate evaluated by CyQuant assay 48 h after treatment and KI-67 expression analysed by RT-qPCR ( $n = 4$  per condition). (C) RT-qPCR for *EGR2*, *PLP1* and *PMP22* analysed in hTERT NF1 cells treated 48 h with hsGDF5 or PBS ( $n = 4$  per condition). (D) Graphical representation of *in vitro* experiment (created with BioRender.com) using human differentiated muscle cells (8220) treated 72 h with hsGDF5 (50 ng/ml) or PBS (control). RT-qPCR for *MuRF1* was performed in 8220 cells treated 72 h with hsGDF5 or PBS ( $n = 3$  per condition). All data are shown as the mean  $\pm$  standard error of the mean. \* $P < 0.05$ , \*\* $P < 0.01$ , \*\*\* $P < 0.001$ . (A and D)  $P$ -values were calculated by unpaired  $t$ -test or (B and C) by ordinary one-way ANOVA followed by Dunnett's multiple comparison test.

apelin and follistatin levels (Fig. 6B) in old, treated TAs, confirming the ability of GDF5 to promote these markers and myokine expression.

The efficacy of chronic rGDF5 treatment was evaluated by MRI measurement, an *in vivo* outcome applicable to future clinical studies. We found that total hind limb muscle CSA was higher after

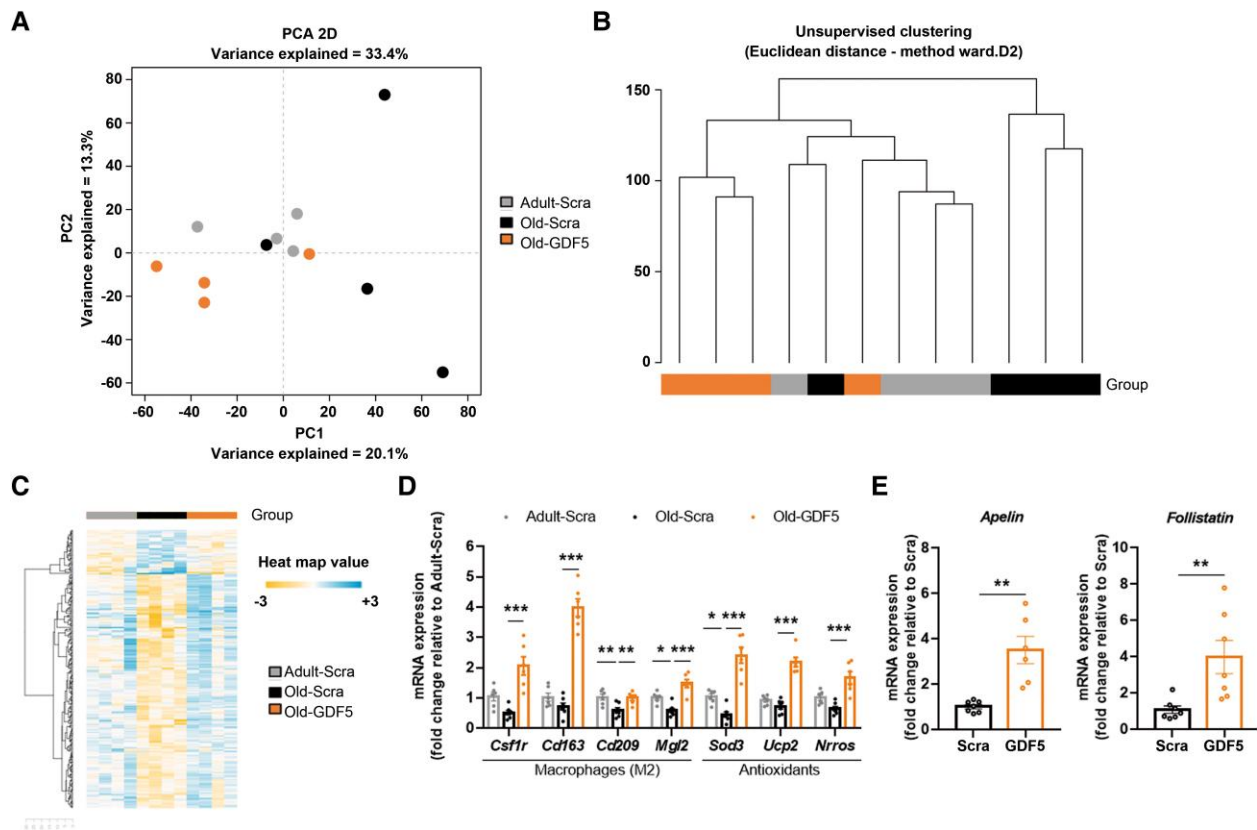


**Figure 5** GDF5 overexpression rejuvenates old whole muscle transcriptomic profile. (A) Principal component analysis (PCA) for gene expression patterns analysed in tibialis anterior (TA) from 7-month adult and 21-month-old mice injected with AAV-Scramble (Adult-Scra  $n=4$ , Old-Scra;  $n=4$ ) or GDF5 (Old-GDF5;  $n=4$ ). (B) Graphical representation of unsupervised hierarchical sample clustering across groups. (C) Heat map showing 247 dysregulated genes in Old-Scra compared with Adult-Scra, which are normalized in Old-GDF5. (D) Real-time quantitative PCR (RT-qPCR) for *Csf1r*, *Cd163*, *Cd209*, *Mgl2*, *Sod3*, *Ucp2* and *Nrros* analysed in TAs of Adult-Scra ( $n=6$ ), Old-Scra ( $n=7$ ) and Old-GDF5 ( $n=6$ ). (E) RT-qPCR for apelin and follistatin analysed in TAs of Old-Scra ( $n=7$ ) and Old-GDF5 ( $n=6-7$ ). All data are shown as the mean  $\pm$  standard error of the mean. \* $P < 0.05$ , \*\* $P < 0.01$ , \*\*\*\* $P < 0.001$ . (D)  $P$ -values were calculated by ordinary one-way ANOVA followed by Dunnett's multiple comparison test or (E) by unpaired  $t$ -test.

treatment compared with the vehicle condition. Accordingly, GAS, TA, EDL and SOL muscle masses were higher in very old mice (24 months) after rGDF5 versus vehicle treatment. Histological analysis of the GAS revealed that this increase was not due to changes in fibre number (Fig. 6C) but increased MyHC-IIB- and MyHC-IIX-positive fibre size (Fig. 6D), rescuing their age-related phenotype. rGDF5 effect on muscle mass was independent of body weight as a slight effect was observed on body composition of fat and lean mass ( $P=0.4919$  and  $P=0.2366$ , respectively) (Supplementary Fig. 6B). The metabolic phenotyping showed that rGDF5 treatment did not affect food and water intake, ambulatory activity nor energy expenditure or respiratory rate. Furthermore, we did not detect modifications in heart weight (Supplementary Fig. 6D) or function measured by ECG (Supplementary Table 5). Considering the impact of GDF5 on bone homeostasis,<sup>26</sup> we measured *ex vivo* femur microarchitecture by micro-CT imaging and did not observe any difference between rGDF5 and vehicle-treated groups (Supplementary Fig. 6E).

Chronic rGDF5 administration effects on muscle function were evaluated by *in situ* TA force generation, which showed increases in both absolute and specific force and a significantly higher rate of force generation versus vehicle ( $P=0.0006$ ) (Fig. 6E), indicating ameliorated neuromuscular connectivity. NMJ morphological analysis revealed no difference in nerve terminal area, overlap percentage, compactness and AChR

fragmentation; however, rGDF5 treatment led to higher endplate and AChR areas in very old mice ( $P=0.0211$  and  $0.0125$ , respectively) (Fig. 6F).

In summary, our findings demonstrate the effectiveness of chronic rGDF5 administration in counteracting age-related muscle wasting, improving muscle function, ensuring neuromuscular connectivity and preventing NMJ instability.

## Discussion

Sarcopenia, a widespread age-related disease strongly impacting life quality and representing a public health issue, is a multifactorial pathology with no cure to date. Here, we aimed at identifying a potential therapeutic strategy for this disease by deciphering the mechanisms underlying GDF5 ability to preserve aged muscle. Our data support its major dual action on both skeletal muscle and NMJs at the earlier stage of ageing, by increasing muscle mass, ameliorating neuromuscular connectivity and endplate structure. We dissected the effect of GDF5 on different pathways as protein synthesis/degradation, innervation and potential mechanisms related to inflammation, metabolism and redox equilibrium. We confirmed that GDF5-OE reduces the expression MuRF1, involved in protein breakdown,<sup>23</sup> and increases protein synthesis. While muscle wasting was likely prevented by rebalanced protein catabolism, the canonical protein synthesis-associated pathway was not affected, consistent

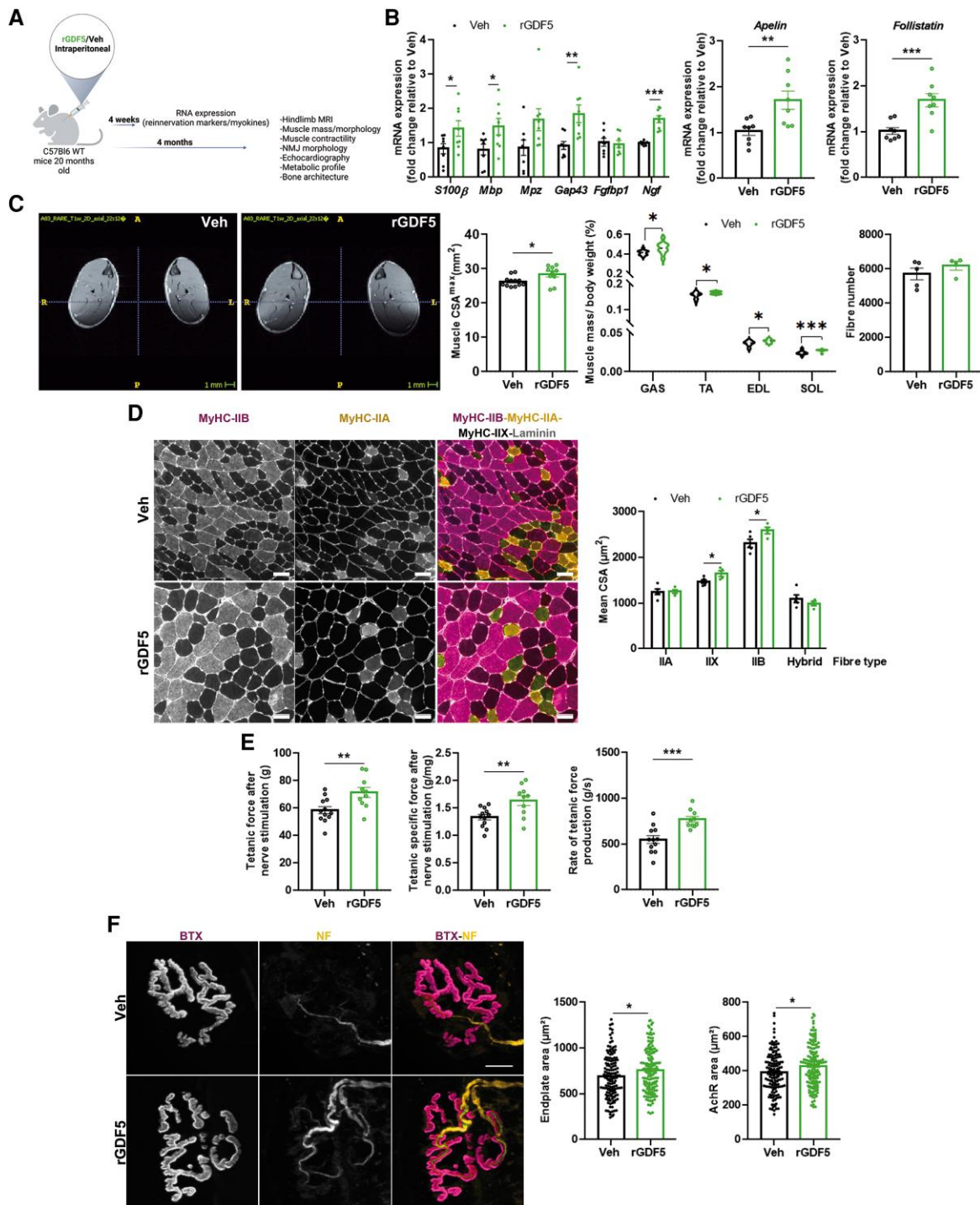


**Figure 6** Chronic rGDF5 systemic administration in ageing mice preserves against age-related muscle wasting and improves neuromuscular junction morphology. (A) Graphical representation of *in vivo* experimental design (created with BioRender.com). Recombinant mouse GDF5 (rGDF5) or control vehicle (Veh) were administered intraperitoneally into 20-month-old mice. Four weeks after repetitive injections, gene expression was analysed in tibialis anterior (TA) and the therapeutic effect was evaluated 4 months after the beginning of the treatment. (B) RT-qPCR for *S100β*, *Mbp*, *Mpz*, *Pmp22*, *Gap-43*, *Fgfbp1*, *Ngf*, *Apelin* and *Follistatin* analysed in TAs of mice treated for 4 weeks with Veh ( $n=8$ ) or rGDF5 ( $n=8$ ). (C) Quantification of maximal muscle cross-sectional area (CSA) determined by MRI in hind limbs of mice treated for 4 months with Veh ( $n=12$ ) or rGDF5 ( $n=10$ ); scale bar = 1 mm. Muscle/body weight ratio of gastrocnemius (GAS), TA, extensor digitorum longus (EDL) and soleus (SOL) of mice treated for 4 months with Veh ( $n=12$ ) or rGDF5 ( $n=10$ ). Mean myofiber number was determined in GAS of mice treated for 4 months with Veh ( $n=5$ ) or rGDF5 ( $n=4$ ). (D) Representative images of GAS cryosections immunostained with laminin (staining membrane), MyHC-IIB (staining type IIB fibres), MyHC-IIA (staining type IIA fibres) and MyHC-IIX (staining type IIX fibres). Hybrid MyHC fibres express both MyHC-IIB and MyHC-IIA, MyHC-I expressing fibres are absent in GAS; scale bar = 100  $\mu\text{m}$ . Mean of myofiber CSA for each fibre type was determined in GAS of mice treated with Veh ( $n=5$ ) or rGDF5 ( $n=4$ ) using ImageJ-based machine learning algorithm. (E) Absolute tetanic force, specific force and rate of force production measured in TAs from mice treated with Veh ( $n=12$ ) or rGDF5 ( $n=10$ ). (F) Representative images of NMJ from EDLs immunostained with neurofilament (NF: staining nerve terminal) and bungarotoxin (BTX: staining acetylcholine receptor); scale bar = 10  $\mu\text{m}$ . Endplate area and acetylcholine receptor (AChR) area parameters were determined in mice treated with Veh ( $n=4$ ) or rGDF5 ( $n=5$ ). All data are shown as the mean  $\pm$  standard error of the mean. \* $P < 0.05$ , \*\* $P < 0.01$ , \*\*\* $P < 0.001$ . (A and E)  $P$ -values were calculated by unpaired  $t$ -test or (F) by Mann-Whitney test.

with previous observations indicating transient/limited impact of Akt/mTor signalling on muscle mass preservation in different conditions.<sup>88–90</sup>

Regarding muscle innervation parameters, we showed that GDF5-OE induced the expression of nerve regeneration- and SC-related reinnervation genes. This finding is consistent with other studies showing GDF5 as a neurotrophic factor protecting dopaminergic neurons from neurotoxicity *in vitro* and *in vivo*<sup>32,91</sup> and promoting neurite complexity in cultured neurons.<sup>92,93</sup> However, we pointed out a more prominent effect of this factor on SCs, essential for NMJ integrity and neuromuscular maintenance,<sup>6</sup> which are affected by ageing.<sup>8</sup>

Overall, our data demonstrated GDF5 rejuvenating effects with reversed expression of several genes altered in aged muscle, particularly those linked to impaired inflammation, macrophages and oxidative balance. Indeed, the steadiness between ATP/heat productions is crucial to regulating ROS production rates for tissue maintenance. In this context, UCPs, which have a physiological role in dissipating energy by decreasing mitochondrial membrane potential, are of interest. Mitochondrial uncoupling reduces free radical generation and has a protective function in several tissues.<sup>94–98</sup> Notably, UCP2 expression, upregulated by GDF5, has been described to correlate with lifespan in humans.<sup>78,99</sup> Here, we showed that mitochondrial content and morphology were not modified and that metabolic phenotyping was also unaffected by GDF5 treatment. However, additional extensive studies are needed to analyse further the possible impact of GDF5-based treatment on the bioenergetics and redox capacity of muscle and their eventual relationship to performance and mass homeostasis. Furthermore, macrophages, essential in muscle regeneration,<sup>100,101</sup> are altered during ageing,<sup>70,71</sup> contributing to inadequate repair and muscle wasting.<sup>102</sup> The expression of other markers associated with both macrophages and antioxidant responses, yet not significantly modified during early ageing, was increased upon GDF5-OE, suggesting that it positively modulates inflammation and redox equilibrium. Noteworthy, a beneficial effect similar to that observed upon physical exercise in humans<sup>103–105</sup> has been induced by GDF5-OE, such as increased expression of the myokines apelin and follistatin. Functions and modulations of these factors have only been explored partially thus far,<sup>106–108</sup> and despite their apparent trophic effect in neuromuscular systems,<sup>17,82,109–111</sup> evidence of their molecular triggers is lacking.<sup>17,110,112</sup>

We addressed the challenge of developing a therapeutic approach using systemic rGDF5 administration, uncovering promising data on its benefits against sarcopenia. We revealed the efficacy of hsGDF5 in human cells in promoting nerve regeneration/reinnervation markers and proliferation of SCs, found to be decreased in aged human muscle, indicating a potential medical use. In addition, we confirmed the inhibition of MuRF1 expression in human myotubes.

Here, we provide bases for effective medical approaches to ageing muscle and strongly suggest that the therapeutic potential of GDF5 is not limited to sarcopenia but applicable to neuromuscular disorders involving SC degeneration and NMJ dismantling, as in motor neuron diseases (amyotrophic lateral sclerosis, spinal muscular atrophy) and demyelinating neuropathies. Consistently, SMAD1/5-dependent pathway activation has been described as beneficial for motor neuron dysfunction in a *Drosophila* model of amyotrophic lateral sclerosis.<sup>113</sup> In addition, we show that GDF5 influences macrophages, inflammation and oxidative balance, disclosing its possible benefit in several conditions, considering that altered inflammatory responses and oxidative stress play a key

role in muscle wasting following critical illness, cancer cachexia, and immobilization but also in muscular and neuromuscular diseases, including muscular dystrophies.<sup>114–118</sup>

Overall, our results establish that the effects of GDF5 might be exploited for the treatment of different pathological conditions affecting the neuromuscular system as a whole.

## Data availability

The authors confirm that the data supporting the findings of this study are available within the article and its [Supplementary material](#).

## Acknowledgements

We thank A. Lacombe for expertise in indirect calorimetry experiments; B. Matot for MRI analysis; S. Vasseur and M. Chapart for collecting human muscles at Myology Institute Myobank; P. Meunier and S. Benkhelifa-Ziyyat from the MyoVector technical platform of the Centre of Research in Myology-UMRS974 (Paris, France) for AAV production; Y. Marie for RNA sequencing; S. Rosanna Casati and C. De Palma for expertise in mitochondria field; I. Akrouf, N. Vignier and V. Allamand for helpful technical advice; Inovarian for technical service; P. Smeriglio and L. Giordani for scientific discussions.

## Funding

Institut de Myologie (to F.P.R. and S.F.), and Association Française contre les myopathies (to F.P.R. and S.F.).

## Competing interests

The authors declare that they have no competing interests.

## Supplementary material

[Supplementary material](#) is available at *Brain* online.

## References

1. Cruz-Jentoft AJ, Bahat G, Bauer J, et al. Sarcopenia: Revised European consensus on definition and diagnosis. *Age Ageing*. 2019;48:601.
2. Spendiff S, Vuda M, Gouspillou G, et al. Denervation drives mitochondrial dysfunction in skeletal muscle of octogenarians. *J Physiol (Lond)*. 2016;594:7361–7379.
3. Gouspillou G, Picard M, Godin R, Burelle Y, Hepple RT. Role of peroxisome proliferator-activated receptor gamma coactivator 1-alpha (PGC-1 $\alpha$ ) in denervation-induced atrophy in aged muscle: Facts and hypotheses. *Longev Healthspan*. 2013;2:13.
4. Piasecki M, Ireland A, Piasecki J, et al. Failure to expand the motor unit size to compensate for declining motor unit numbers distinguishes sarcopenic from non-sarcopenic older men. *J Physiol (Lond)*. 2018;596:1627–1637.
5. Chai RJ, Vukovic J, Dunlop S, Grounds MD, Shavlakadze T. Striking denervation of neuromuscular junctions without lumbar motoneuron loss in geriatric mouse muscle. *PLoS ONE*. 2011;6:e28090.
6. Jablonka-Shariff A, Lu C-Y, Campbell K, Monk KR, Snyder-Warwick AK. Gpr126/adgrg6 contributes to the

- terminal Schwann cell response at the NMJ following peripheral nerve injury. *Glia*. 2020;68:1182-1200.
7. Fuertes-Alvarez S, Izeta A. Terminal Schwann cell aging: Implications for age-associated neuromuscular dysfunction. *Aging Dis*. 2021;12:494-514.
  8. Ludatscher RM, Silbermann M, Gershon D, Reznick A. Evidence of Schwann cell degeneration in the aging mouse motor endplate region. *Exp Gerontol*. 1985;20:81-91.
  9. Snyder-Warwick AK, Satoh A, Santosa KB, Imai S, Jablonka-Shariff A. Hypothalamic sirt1 protects terminal Schwann cells and neuromuscular junctions from age-related morphological changes. *Aging Cell*. 2018;17:e12776.
  10. Aare S, Spendiff S, Vuda M, et al. Failed reinnervation in aging skeletal muscle. *Skelet Muscle*. 2016;6:29.
  11. Dalle S, Rossmeislova L, Kopko K. The role of inflammation in age-related sarcopenia. *Front Physiol*. 2017;8:1045.
  12. Fulle S, Protasi F, Di Tano G, et al. The contribution of reactive oxygen species to sarcopenia and muscle ageing. *Exp Gerontol*. 2004;39:17-24.
  13. Valdez G, Tapia JC, Kang H, et al. Attenuation of age-related changes in mouse neuromuscular synapses by caloric restriction and exercise. *Proc Natl Acad Sci USA*. 2010;107:14863-14868.
  14. Kern H, Hofer C, Loeffler S, et al. Atrophy, ultra-structural disorders, severe atrophy and degeneration of denervated human muscle in SCI and aging. Implications for their recovery by functional electrical stimulation, updated 2017. *Neurol Res*. 2017;39:660-666.
  15. Kern H, Barberi L, Löfler S, et al. Electrical stimulation counteracts muscle decline in seniors. *Front Aging Neurosci*. 2014;6:189.
  16. Mosole S, Carraro U, Kern H, et al. Long-term high-level exercise promotes muscle reinnervation with age. *J Neuropathol Exp Neurol*. 2014;73:284-294.
  17. Vinel C, Lukjanenko L, Batut A, et al. The exerkine apelin reverses age-associated sarcopenia. *Nat Med*. 2018;1:1360-1371.
  18. Kim JW, Kim R, Choi H, Lee S-J, Bae G-U. Understanding of sarcopenia: From definition to therapeutic strategies. *Arch Pharm Res*. 2021;44:876-889.
  19. Lee S-J. Targeting the myostatin signaling pathway to treat muscle loss and metabolic dysfunction. *J Clin Invest*. 2021;131:10.1172/JCI148372.
  20. Rooks D, Swan T, Goswami B, et al. Bimagrumab vs optimized standard of care for treatment of sarcopenia in community-dwelling older adults: A randomized clinical trial. *JAMA Network Open*. 2020;3:e2020836.
  21. Tournadre A, Vial G, Capel F, Soubrier M, Boirie Y. Sarcopenia. *Joint Bone Spine*. 2019;86:309-314.
  22. Macpherson PCD, Farshi P, Goldman D. Dach2-Hdac9 signaling regulates reinnervation of muscle endplates. *Development*. 2015;142:4038-4048.
  23. Sartori R, Schirwis E, Blaauw B, et al. BMP signaling controls muscle mass. *Nat Genet*. 2013;45:1309-1318.
  24. Traoré M, Gentil C, Benedetto C, et al. An embryonic CaVβ1 isoform promotes muscle mass maintenance via GDF5 signaling in adult mouse. *Sci Transl Med*. 2019;11:eaaw1131.
  25. Chijimatsu R, Saito T. Mechanisms of synovial joint and articular cartilage development. *Cell Mol Life Sci*. 2019;76:3939-3952.
  26. Jin L, Li X. Growth differentiation factor 5 regulation in bone regeneration. *Curr Pharm Des*. 2013;19:3364-3373.
  27. Farooq M, Nakai H, Fujimoto A, et al. Characterization of a novel missense mutation in the prodomain of GDF5, which underlies brachydactyly type C and mild grebe type chondrodysplasia in a large Pakistani family. *Hum Genet*. 2013;132:1253-1264.
  28. Reynard LN, Bui C, Syddall CM, Loughlin J. CpG methylation regulates allelic expression of GDF5 by modulating binding of SP1 and SP3 repressor proteins to the osteoarthritis susceptibility SNP rs143383. *Hum Genet*. 2014;133:1059-1073.
  29. Jones G, Trajanoska K, Santanasto AJ, et al. Genome-wide meta-analysis of muscle weakness identifies 15 susceptibility loci in older men and women. *Nat Commun*. 2021;12:654.
  30. David L, Feige J-J, Bailly S. Emerging role of bone morphogenetic proteins in angiogenesis. *Cytokine Growth Factor Rev*. 2009;20:203-212.
  31. Sullivan AM, O'Keeffe GW. The role of growth/differentiation factor 5 (GDF5) in the induction and survival of midbrain dopaminergic neurones: Relevance to Parkinson's disease treatment. *J Anat*. 2005;207:219-226.
  32. Sullivan AM, Opacka-Juffry J, Pohl J, Blunt SB. Neuroprotective effects of growth/differentiation factor 5 depend on the site of administration. *Brain Res*. 1999;818:176-179.
  33. Sattiel AR. New therapeutic approaches for the treatment of obesity. *Sci Transl Med*. 2016;8:323rv2-323rv2.
  34. Hinoi E, Nakamura Y, Takada S, et al. Growth differentiation factor-5 promotes brown adipogenesis in systemic energy expenditure. *Diabetes*. 2014;63:162-175.
  35. Hegarty SV, Collins LM, Gavin AM, et al. Canonical BMP-smad signalling promotes neurite growth in rat midbrain dopaminergic neurons. *Neuromolecular Med*. 2014;16:473-489.
  36. Sartori R, Hagg A, Zampieri S, et al. Perturbed BMP signaling and denervation promote muscle wasting in cancer cachexia. *Sci Transl Med*. 2021;13:eaay9592.
  37. Stantzou A, Schirwis E, Swist S, et al. BMP signaling regulates satellite cell-dependent postnatal muscle growth. *Development*. 2017;144:2737-2747.
  38. Uezumi A, Ikemoto-Uezumi M, Zhou H, et al. Mesenchymal Bmp3b expression maintains skeletal muscle integrity and decreases in age-related sarcopenia. *J Clin Invest*. 2021;131:e139617.
  39. Sader F, Roy S. Tgf-β superfamily and limb regeneration: Tgf-β to start and bmp to end. *Dev Dyn*. 2022;251:973-987.
  40. Winbanks CE, Chen JL, Qian H, et al. The bone morphogenetic protein axis is a positive regulator of skeletal muscle mass. *J Cell Biol*. 2013;203:345-357.
  41. McPhee JS, Hogrel J-Y, Maier AB, et al. Physiological and functional evaluation of healthy young and older men and women: Design of the European MyoAge study. *Biogerontology*. 2013;14:325-337.
  42. Mamchaoui K, Trollet C, Bigot A, et al. Immortalized pathological human myoblasts: Towards a universal tool for the study of neuromuscular disorders. *Skelet Muscle*. 2011;1:34.
  43. Rivière C, Danos O, Douar AM. Long-term expression and repeated administration of AAV type 1, 2 and 5 vectors in skeletal muscle of immunocompetent adult mice. *Gene Ther*. 2006;13:1300-1308.
  44. Schmidt EK, Clavarino G, Ceppi M, Pierre P. SUNSET, a nonradioactive method to monitor protein synthesis. *Nat Methods*. 2009;6:275-277.
  45. Goodman CA, Mabrey DM, Frey JW, et al. Novel insights into the regulation of skeletal muscle protein synthesis as revealed by a new nonradioactive in vivo technique. *FASEB J*. 2010;25:1028-1039.
  46. Boëx M, Cottin S, Halliez M, et al. The cell polarity protein vangl2 in the muscle shapes the neuromuscular synapse by binding to and regulating the tyrosine kinase MuSK. *Sci Signal*. 2022;15:eabg4982.

47. Yushkevich PA, Piven J, Hazlett HC, et al. User-guided 3D active contour segmentation of anatomical structures: Significantly improved efficiency and reliability. *Neuroimage*. 2006;31:1116-1128.
48. Sheth KA, Iyer CC, Wier CG, et al. Muscle strength and size are associated with motor unit connectivity in aged mice. *Neurobiol Aging*. 2018;67:128-136.
49. Wu G, Xu S, Chen B, Wu P. Relationship between changes in muscle fibers and CMAP in skeletal muscle with different stages of aging. *Int J Clin Exp Pathol*. 2017;10:11888-11895.
50. Sun Y-B, Lou F, Edman KaP. The effects of 2,3-butanedione monoxime (BDM) on the force-velocity relation in single muscle fibres of the frog. *Acta Physiol Scand*. 1995;153:325-334.
51. Nakahiro T, Kurooka H, Mori K, Sano K, Yokota Y. Identification of BMP-responsive elements in the mouse id2 gene. *Biochem Biophys Res Commun*. 2010;399:416-421.
52. Bradford STJ, Ranghini EJ, Grimley E, Lee PH, Dressler GR. High-throughput screens for agonists of bone morphogenetic protein (BMP) signaling identify potent benzoxazole compounds. *J Biol Chem*. 2019;294:3125-3136.
53. Zammit PS, Partridge TA, Yablonka-Reuveni Z. The skeletal muscle satellite cell: The stem cell that came in from the cold. *J Histochem Cytochem*. 2006;54:1177-1191.
54. Sartori R, Gregorevic P, Sandri M. TGF $\beta$  and BMP signaling in skeletal muscle: Potential significance for muscle-related disease. *Trends Endocrinol Metab*. 2014;25:464-471.
55. Blaauw B, Canato M, Agatea L, et al. Inducible activation of Akt increases skeletal muscle mass and force without satellite cell activation. *FASEB J*. 2009;23:3896-3905.
56. Peris-Moreno D, Taillandier D, Polge C. MuRF1/TRIM63, master regulator of muscle mass. *Int J Mol Sci*. 2020;21:6663.
57. Cohen S, Brault JJ, Gygi SP, et al. During muscle atrophy, thick, but not thin, filament components are degraded by MuRF1-dependent ubiquitylation. *J Cell Biol*. 2009;185:1083-1095.
58. Liang Q, Cai M, Zhang J, et al. Role of muscle-specific histone methyltransferase (smyd1) in exercise-induced cardioprotection against pathological remodeling after myocardial infarction. *Int J Mol Sci*. 2020;21:7010.
59. Kitajima Y, Suzuki N, Yoshioka K, et al. Inducible rpt3, a proteasome component, knockout in adult skeletal muscle results in muscle atrophy. *Front Cell Dev Biol*. 2020;8:859.
60. Chen S, Chen J, Wang C, et al. Betaine attenuates age-related suppression in autophagy via Mettl21c/p97/VCP axis to delay muscle loss. *J Nutr Biochem*. 2023;125:109555.
61. Chen Y, Ma Y, Tang J, et al. Physical exercise attenuates age-related muscle atrophy and exhibits anti-ageing effects via the adiponectin receptor 1 signalling. *J Cachexia Sarcopenia Muscle*. 2023;14:1789-1801.
62. Piétri-Rouxel F, Gentil C, Vassilopoulos S, et al. DHPK  $\alpha$ 1s subunit controls skeletal muscle mass and morphogenesis. *EMBO J*. 2010;29:643-654.
63. Peczkowski KK, Rastogi N, Lowe J, et al. Muscle twitch kinetics are dependent on muscle group, disease state, and age in duchenne muscular dystrophy mouse models. *Front Physiol*. 2020;11:1203.
64. Jones RA, Reich CD, Dissanayake KN, et al. NMJ-morph reveals principal components of synaptic morphology influencing structure-function relationships at the neuromuscular junction. *Open Biol*. 2016;6:160240.
65. Shadrach JL, Pierchala BA. Semaphorin3A signaling is dispensable for motor axon reinnervation of the adult neuromuscular junction. *eNeuro*. 2018;5:ENEURO.0155-17.2018.
66. Davis-Lopez de Carrizosa MA, Morado-Diaz CJ, Morcuende S, de la Cruz RR, Pastor AM. Nerve growth factor regulates the firing patterns and synaptic composition of motoneurons. *J Neurosci*. 2010;30:8308-8319.
67. Höke A, Redett R, Hameed H, et al. Schwann cells express motor and sensory phenotypes that regulate axon regeneration. *J Neurosci*. 2006;26:9646-9655.
68. Taetzsch T, Tenga MJ, Valdez G. Muscle fibers secrete FGFBP1 to slow degeneration of neuromuscular synapses during aging and progression of ALS. *J Neurosci*. 2017;37:70-82.
69. Barik A, Li L, Sathyamurthy A, Xiong W-C, Mei L. Schwann cells in neuromuscular junction formation and maintenance. *J Neurosci*. 2016;36:9770-9781.
70. Kawanishi N, Machida S. Alterations of macrophage and neutrophil content in skeletal muscle of aged versus young mice. *Muscle Nerve*. 2021;63:600-607.
71. Cui C-Y, Driscoll RK, Piao Y, Chia CW, Gorospe M, Ferrucci L. Skewed macrophage polarization in aging skeletal muscle. *Aging Cell*. 2019;18:e13032.
72. Zhao R-Z, Jiang S, Zhang L, Yu Z-B. Mitochondrial electron transport chain, ROS generation and uncoupling (review). *Int J Mol Med*. 2019;44:3-15.
73. Börsch A, Ham DJ, Mittal N, et al. Molecular and phenotypic analysis of rodent models reveals conserved and species-specific modulators of human sarcopenia. *Commun Biol*. 2021;4:1-15.
74. Grabert K, Sehgal A, Irvine KM, et al. A transgenic line that reports CSF1R protein expression provides a definitive marker for the mouse mononuclear phagocyte system. *J Immunol*. 2020;205:3154-3166.
75. Walton RG, Kosmac K, Mula J, et al. Human skeletal muscle macrophages increase following cycle training and are associated with adaptations that may facilitate growth. *Sci Rep*. 2019;9:969.
76. Shook BA, Wasko RR, Rivera-Gonzalez GC, et al. Myofibroblast proliferation and heterogeneity are supported by macrophages during skin repair. *Science*. 2018;362:eaar2971.
77. Amara CE, Shankland EG, Jubrias SA, Marcinek DJ, Kushmerick MJ, Conley KE. Mild mitochondrial uncoupling impacts cellular aging in human muscles in vivo. *Proc Natl Acad Sci U S A*. 2007;104:1057-1062.
78. Andrews ZB. Uncoupling protein-2 and the potential link between metabolism and longevity. *Curr Aging Sci*. 2010;3:102-112.
79. Rose G, Crocco P, Rango FD, Montesanto A, Passarino G. Further support to the uncoupling-to-survive theory: The genetic variation of human UCP genes is associated with longevity. *PLoS One*. 2011;6:e29650.
80. Cui R, Gao M, Qu S, Liu D. Overexpression of superoxide dismutase 3 gene blocks high-fat diet-induced obesity, fatty liver and insulin resistance. *Gene Ther*. 2014;21:840-848.
81. Noubade R, Wong K, Ota N, et al. NRRROS negatively regulates reactive oxygen species during host defence and autoimmunity. *Nature*. 2014;509:235-239.
82. Iyer CC, Chugh D, Bobbili PJ, et al. Follistatin-induced muscle hypertrophy in aged mice improves neuromuscular junction innervation and function. *Neurobiol Aging*. 2021;104:32-41.
83. Liu X, Zhang N, Sun B, Wang B. Time-specific effects of acute eccentric exercise on myostatin, follistatin and decorin in the circulation and skeletal muscle in rats. *Physiol Res*. 2022;71:783-790.
84. Brandt N, Dethlefsen MM, Bangsbo J, Pilegaard H. PGC-1 $\alpha$  and exercise intensity dependent adaptations in mouse skeletal muscle. *PLoS ONE*. 2017;12:e0185993.
85. Mills R, Taylor-Weiner H, Correia JC, et al. Neurturin is a PGC-1 $\alpha$ -controlled myokine that promotes motor neuron

- recruitment and neuromuscular junction formation. *Mol Metab.* 2017;7:12-22.
86. Vue Z, Garza-Lopez E, Neikirk K, et al. 3D reconstruction of murine mitochondria reveals changes in structure during aging linked to the MICOS complex. *Aging Cell.* 2023;22:e14009.
  87. De Palma C, Falcone S, Pisoni S, et al. Nitric oxide inhibition of drp1-mediated mitochondrial fission is critical for myogenic differentiation. *Cell Death Differ.* 2010;17:1684-1696.
  88. Roy A, Kumar A. Supraphysiological activation of TAK1 promotes skeletal muscle growth and mitigates neurogenic atrophy. *Nat Commun.* 2022;13:2201.
  89. Baehr LM, West DWD, Marcotte G, et al. Age-related deficits in skeletal muscle recovery following disuse are associated with neuromuscular junction instability and ER stress, not impaired protein synthesis. *Aging (Albany NY).* 2016;8:127-146.
  90. Sandri M, Barberi L, Bijlsma AY, et al. Signalling pathways regulating muscle mass in ageing skeletal muscle. The role of the IGF1-akt-mTOR-FoxO pathway. *Biogerontology.* 2013;14:303-323.
  91. Hurley FM, Costello DJ, Sullivan AM. Neuroprotective effects of delayed administration of growth/differentiation factor-5 in the partial lesion model of Parkinson's disease. *Exp Neurol.* 2004;185:281-289.
  92. Hegarty SV, O'Keeffe GW, Sullivan AM. BMP-Smad 1/5/8 signaling in the development of the nervous system. *Prog Neurobiol.* 2013;109:28-41.
  93. Osório C, Chacón PJ, Kisiswa L, et al. Growth differentiation factor 5 is a key physiological regulator of dendrite growth during development. *Development.* 2013;140:4751-4762.
  94. Normoyle KP, Kim M, Farahvar A, Llano D, Jackson K, Wang H. The emerging neuroprotective role of mitochondrial uncoupling protein-2 in traumatic brain injury. *Transl Neurosci.* 2015;6:179-186.
  95. Robbins D, Zhao Y. New aspects of mitochondrial uncoupling proteins (UCPs) and their roles in tumorigenesis. *Int J Mol Sci.* 2011;12:5285-5293.
  96. de Oliveira Bristot VJ, de Bem Alves AC, Cardoso LR, da Luz Scheffer D, Aguiar AS. The role of PGC-1 $\alpha$ /UCP2 signaling in the beneficial effects of physical exercise on the brain. *Front Neurosci.* 2019;13:292.
  97. Montez P, Vázquez-Medina JP, Rodríguez R, et al. Angiotensin receptor blockade recovers hepatic UCP2 expression and aconitase and SDH activities and ameliorates hepatic oxidative damage in insulin resistant rats. *Endocrinology.* 2012;153:5746-5759.
  98. Sullivan PG, Dubé C, Dorenbos K, Steward O, Baram TZ. Mitochondrial uncoupling protein-2 protects the immature brain from excitotoxic neuronal death. *Ann Neurol.* 2003;53:711-717.
  99. Dietrich MO, Horvath TL. The role of mitochondrial uncoupling proteins in lifespan. *Pflugers Arch.* 2010;459:269-275.
  100. Rigamonti E, Zordan P, Sciorati C, Rovere-Querini P, Brunelli S. Macrophage plasticity in skeletal muscle repair. *Biomed Res Int.* 2014;2014:e560629.
  101. Roux-Biejat P, Coazzoli M, Marrazzo P, et al. Acid sphingomyelinase controls early phases of skeletal muscle regeneration by shaping the macrophage phenotype. *Cells.* 2021;10:3028.
  102. van Beek AA, Van den Bossche J, Mastroberardino PG, de Winther MPJ, Leenen PJM. Metabolic alterations in aging macrophages: Ingredients for inflammaging? *Trends Immunol.* 2019;40:113-127.
  103. Hangelbroek RWJ, Fazlzadeh P, Tieland M, et al. Expression of protocadherin gamma in skeletal muscle tissue is associated with age and muscle weakness. *J Cachexia Sarcopenia Muscle.* 2016;7:604-614.
  104. Lavin KM, Perkins RK, Jemiolo B, Raue U, Trappe SW, Trappe TA. Effects of aging and lifelong aerobic exercise on basal and exercise-induced inflammation in women. *J Appl Physiol (1985).* 2020;129:1493-1504.
  105. Raue U, Trappe TA, Estrem ST, et al. Transcriptome signature of resistance exercise adaptations: Mixed muscle and fiber type specific profiles in young and old adults. *J Appl Physiol (1985).* 2012;112:1625-1636.
  106. Armand A-S, Della Gaspera B, Launay T, Charbonnier F, Gallien CL, Chanoine C. Expression and neural control of follistatin versus myostatin genes during regeneration of mouse soleus. *Dev Dyn.* 2003;227:256-265.
  107. Bagheri R, Moghadam BH, Church DD, et al. The effects of concurrent training order on body composition and serum concentrations of follistatin, myostatin and GDF11 in sarcopenic elderly men. *Exp Gerontol.* 2020;133:110869.
  108. Ivanov MN, Stoyanov DS, Pavlov SP, Tonchev AB. Distribution, function, and expression of the apelinergic system in the healthy and diseased mammalian brain. *Genes (Basel).* 2022;13:2172.
  109. Chugh D, Iyer CC, Bobbili P, et al. Voluntary wheel running with and without follistatin overexpression improves NMJ transmission but not motor unit loss in late life of C57BL/6J mice. *Neurobiol Aging.* 2021;101:285-296.
  110. Kwak SE, Cho SC, Bae JH, et al. Effects of exercise-induced apelin on muscle function and cognitive function in aged mice. *Exp Gerontol.* 2019;127:110710.
  111. Kasai A, Kinjo T, Ishihara R, et al. Apelin deficiency accelerates the progression of amyotrophic lateral sclerosis. *PLoS One.* 2011;6:e23968.
  112. Hofmann M, Schober-Halper B, Oesen S, et al. Effects of elastic band resistance training and nutritional supplementation on muscle quality and circulating muscle growth and degradation factors of institutionalized elderly women: The Vienna active ageing study (VAAS). *Eur J Appl Physiol.* 2016;116:885-897.
  113. Held A, Major P, Sahin A, Reenan RA, Lipscombe D, Wharton KA. Circuit dysfunction in SOD1-ALS model first detected in sensory feedback prior to motor neuron degeneration is alleviated by BMP signaling. *J Neurosci.* 2019;39:2347-2364.
  114. Guttenplan KA, Weigel MK, Adler DI, et al. Knockout of reactive astrocyte activating factors slows disease progression in an ALS mouse model. *Nat Commun.* 2020;11:3753.
  115. Brohawn DG, O'Brien LC, Bennett JP. RNAseq analyses identify tumor necrosis factor-mediated inflammation as a Major abnormality in ALS spinal cord. *PLoS One.* 2016;11:e0160520.
  116. Bouredji Z, Argaw A, Frenette J. The inflammatory response, a mixed blessing for muscle homeostasis and plasticity. *Front Physiol.* 2022;13:1032450.
  117. Park HT, Kim YH, Lee KE, Kim JK. Behind the pathology of macrophage-associated demyelination in inflammatory neuropathies: Demyelinating Schwann cells. *Cell Mol Life Sci.* 2020;77:2497-2506.
  118. Ransohoff RM. How neuroinflammation contributes to neurodegeneration. *Science.* 2016;353:777-783.